SAKARYA ÜNİVERSİTESİ
FEN BİLİMLERİ ENSTİTÜSÜ DERGİSİ

Sakarya University Journal of Science
SAUJS

ISSN 1301-4048 e-ISSN 2147-835X Period Bimonthly Founded 1997 Publisher Sakarya University
http://www.saujs.sakarya.edu.tr/

Title: Electrospun PVDF Membranes Incorporated with Functionalized Carbon-based Material for Removal of Cationic Dyes

Authors: Fatma DEMİRCİ, Burçak KAYA ÖZSEL

Recieved: 2022-10-27 00:00:00

Accepted: 2023-01-31 00:00:00

Article Type: Research Article

Volume: 27
Issue: 2
Month: April
Year: 2023
Pages: 386-397

How to cite
Fatma DEMİRCİ, Burçak KAYA ÖZSEL; (2023), Electrospun PVDF Membranes Incorporated with Functionalized Carbon-based Material for Removal of Cationic Dyes . Sakarya University Journal of Science, 27(2), 386-397, DOI: 10.16984/saufenbilder.1195528
Access link
https://dergipark.org.tr/en/pub/saufenbilder/issue/76551/1195528

Sakarya University Journal of Science 27(2), 386-397, 2023

Electrospun PVDF Membranes Incorporated with Functionalized Carbon-based Material for Removal of Cationic Dyes

Fatma DEMIRCI *[1], Burcak KAYA OZSEL[1]

Abstract

In this study, polyvinylidene fluoride (PVDF) polymeric membranes with addition of functionalized carbon-based material (CBM) were fabricated by using electrospinning technique for the removal of cationic dyes from wastewater. CBM was prepared through a two-step carbonization process from cotton linter as an agricultural waste biomass. The characterization of CBM was performed by using Brunauer–Emmett–Teller (BET) surface analysis, fourier transform infrared spectrometry (FTIR) and elemental analysis. The morphologies of electrospun membranes were observed by scanning electron microscope (SEM) which clearly revealed that nanofibers with a smooth surface were produced by incorporation of CBM. According to the results obtained from FTIR and differential scanning calorimetry (DSC), crystallization behavior of PVDF membranes was promoted by increasing the percentage of CBM in the membrane. PVDF membrane prepared with the addition of 3 wt % CBM exhibited the highest water flux performance with a dye rejection of 74.6 % in comparison with the pure PVDF one.

Keywords: Electrospinning, membrane, carbon-based material, dye removal

1. INTRODUCTION

Water, which is vital for sustaining life, is becoming an increasingly scarce resource due to the constantly increasing industrialization and rapid population growth globally. Namely, billions people do not have access to water and sanitation. One of the most important problem in front of sanitation is organic dyes used in many industries such as textile, food, leather, paper and plastic [1]. It is stated that 100.000 different types of paint are commercially produced for use in these industries, and 10-15% of the paints, which reach an annual production amount of 1.6 million tons, are discharged into the water without being specifically treated [1-3]. Many of these paints mixed with water are toxic and difficult to degrade, thus creating serious problems for aquatic organisms and humans. Therefore, many studies have been carried out to remove these pollutants from water such as advanced oxidation processes [4], membrane filtration [5], photocatalytic oxidation reaction [6], and adsorption [7]. Although membrane technologies are the most preferred method in water applications,

* Corresponding author: fatma.demirci@btu.edu.tr (F.DEMIRCI)
[1] Bursa Technical University
E-mail: burcak.kaya@btu.edu.tr
ORCID: https://orcid.org/0000-0002-0617-8606, http://orcid.org/0000-0003-2190-3834

the adsorption method is considered the most promising method for the removal of organic dyes [2, 8, 9]. In this sense, membrane applications containing adsorbent additives have been studied in the literature recently [10-12].

Electrospinning membranes with high surface area and pore ratio are thought to offer great advantages in environmental applications. PVDF polymer, which is frequently preferred in membrane applications due to its high mechanical strength, thermal and chemical stability, can be easily processed in electrospinning, making the electrospinning process even more usable in membrane applications for water treatments [13-15]. An adsorbent additive to be made into the PVDF membrane will provide a significant efficiency in the removal of dyestuffs in water. In the literature, there are membrane studies in which various adsorbents such as metal-organic frameworks (MOFs) [16, 17], magnetic particles [18], inorganic metal oxides [19], carbon nanotubes [20]. are used. Adding carbon-based materials used as adsorbent into the membrane as an additive will be effective in removing the dyestuff in the water.

Thermal (inert atmosphere, generally ≤ 600 °C) and hydrothermal (in water, generally 180–300 °C) carbonization are known as the common carbonization methods especially to produce biomass-derived carbon materials [21]. The characteristics of biomass-derived carbon structures are directly affected by the carbonization method due to the differences in reaction mechanism during the different carbonization methods. For instance, specific surface areas are generally low for hydrothermally treated biomass-derived carbon materials. There are many reports in the literature about the carbon materials produced by only using a single carbonization method [22, 23]. In the first part of the study, two carbonization processes were applied consecutively to produce carbon structure with superior physical and chemical properties. In both carbonization processes relatively low temperatures were applied to prepare carbon structure with a higher density of acid sites because biomass components are not completely hydrolysed at low temperatures, thus leading to the formation of surface functional groups onto the carbon surface. Also in the thermal carbonization process if the temperature increases, sulfonic functional groups can decompose decreasing the acidic functionalization [24]. Here, sulfamic and citric acid were used in order to accelerate the decomposition of cellulosic biomass and acidic functionalization of carbon structure to improve dye adsorption capacity. Sulfamic acid is a strong (pKa $\approx$ 1), low-cost, low-corrosive, non-toxic acid for functionalization and citric acid is like a catalyst that leads to higher carbon content during carbonization. The acid-functionalized carbon-based material was characterized by using Brunauer–Emmett–Teller (BET) surface analysis, fourier transform infrared spectrometry (FTIR) and elemental analysis.

In the second part of the study, electrospun PVDF membranes were produced by addition of various amounts of the produced CBM. The CBM addition effect on crystallization behavior of PVDF was investigated by FTIR and DSC analyses. It has been demonstrated by SEM images that CBM addition supports nanofiber formation by regulating jet formation. The effect of the additive on the water flux and cationic dye (methylene blue) rejection ratio of the membrane were investigated.

2. MATERIALS and METHOD

2.1. Materials

Cotton linter as a carbon precursor was provided from a local supplier in Adana, Turkey. It has a cellulose content of 83.4 % (w/w) determined by using the method described in the literature [25]. Sulfamic

acid (≥ 99.0 %, Merck, Germany) and citric acid (≥ 99.5 %, Sigma-Aldrich, Germany) were used for effective carbonization and functionalization of carbon-based material. Polyvinylidene fluoride (PVDF) (Solef® 1015- Solvay, Mw=516,000, Alpharetta, GA, USA) powder was used as a base polymer to prepare electrospun membranes. N,N-Dimethylacetamide (DMAc) (Sigma-Aldrich, Germany), acetone and methanol (Merck, Germany) were used as solvents. Methylene Blue (MB) (Sigma, Italy) was used as a model cationic dye.

2.2. Production of Carbon-based Material

Before the hydrothermal carbonization process alkali treatment was carried out to purify linter biomass [26]. 25.0 g raw linter was treated with 5% (w/v) aqueous NaOH solution for 1 h at 70 °C under stirring. Cold distilled water was added to the mixture to stop the reaction and then the mixture was filtered until to reach pH 6. The dried alkali treated linter biomass was bleached with a 1:20 (g/ml) solution of H_2O_2 30% (v/v) for 1 h at 50 °C under constant stirring. Cold distilled water was added to the mixture in order to stop the reaction and then the mixture was vacuum filtered until to reach pH 6. The bleached fibers were dried in an oven for 48 h at 60 °C.

Carbon-based material was prepared by successive hydrothermal and thermal carbonization of cotton linter. In hydrothermal carbonization process, 1.5 g biomass, 1.5 g sulfamic acid and 0.5 g citric acid were mixed with 20 mL water and the mixture pretreated with high power ultrasound for 10 min by using an ultrasonic probe sonicator. Then the slurry was subjected to heat treatment in a teflon sealed autoclave at 180 °C for 20 h. The semi-carbonized solid was washed by DI water and methanol to remove impurities and dried at 100 °C for 24 h. In the thermal carbonization process, hydrothermally treated-solid was transferred in a tube fixed furnace then heated to 300 °C at 5°C/min and held for 3 hours under nitrogen atmosphere. After the tube furnace was cooled to room temperature the solid sample was washed with distilled water and dried at 105 °C for 24 h in an oven. Prepared carbon-based material was labeled as 'CBM'. The CBM was sieved at the particle size below 40 mesh prior to use. For comparison a raw carbon-based material was also prepared without using any acids in the hydrothermal carbonization process, labeled as 'CBM0'. All produced carbon-based materials were stored in a desiccator until use.

2.3. Production of CBM Added Electrospun Membranes

To obtain spinning solution firstly, 18 wt% PVDF was dissolved in a mixed solvent of DMAc and acetone with a weight ratio of 1:1, by stirring at 50 °C for 24 h. Then, various amounts of CBM (1 wt%, 2 wt%, and 3 wt%) were added into the solution and stirring was continued for 1 more hour at room temperature to properly disperse the CBM into the solution. The produced membranes were labeled as M-0 (0 wt% CBM), M-1 (1 wt% CBM), M-2 (2 wt% CBM), and M-3 (3 wt% CBM) depending on the amount of the CBM they contain. 20 mL of the prepared solution was taken in a plastic syringe and electrospun on aluminum sheets at 23-27 kV through an electrospinning device (İnovenso – Nanospinner24). The tip and collector distance was 20 cm and the solution fed ratio was 6 mL/h from a diameter capillary tip 20 mL syringe with 1.36 cm inner diameter.

2.4. Characterization of Carbon-based Material

The total surface area and pore size of the CBM and CBM0 were determined by N_2 adsorption–desorption at 77 K using a Micrometrics TriStar II instrument and prior to the analysis the samples were out gassed for 20 h at 473 K. The C,N,H content of carbon-based materials were determined by

using a Thermo Scientific FlashSmart Elemental Analyzer. Identification of the functional groups on the surface of samples was performed by FTIR spectroscopy (Perkin Elmer Spectrum Two FTIR ATR System). The total acidity of carbon-based materials was determined by the titration method [27].

2.5. Characterization of CBM Added Membranes

The produced membranes were characterized with FTIR (Thermo Nicolet, iS50 with an attenuated total reflectance (ATR) accessory) analyses. The FTIR spectra of the samples were recorded in the wavenumber range 400 to 4,000 cm^{-1} with 16 scans at 4 cm^{-1} resolutions.

Thermal properties of the produced membranes and the effect of the additive on crystallization behavior of the membranes were characterized with differential scanning calorimeter (DSC) (TA Instrument/DSC25) analyses. Membrane samples of 7-8 mg were heated to 200 °C from -90 °C at a heating rate of 10 °C/min under nitrogen atmosphere.

The water flux and MB rejection performances of the produced membranes were measured with a stirred cell (effective area, 14.6 cm^2, HP4750 Sterlitech) at 1 bar pressure. The produced membranes pure water flux values (J_w) ($L/m^2h.bar$) were calculated by the following equation:

$$J_w = \frac{V}{A \times t} \quad (1)$$

where V (L) is the permeated water volume at in the operation time t (h), and A (m^2) is the effective membrane area.

The same cell was used for the MB rejection measurements of the produced membranes. 10 ppm MB was used as feed solution. The concentration of the MB in the feed and permeate were determined with UV-Visible spectrometer (Scinco-NEOSYS200) at 665 nm wavelength. The MB rejection percentage $(R, \%)$ of the produced membranes were determined with following equation:

$$R(\%) = \frac{A_f - A_p}{A_f} \times 100 \quad (2)$$

where the A_f and A_p were the absorbance value of the feed and permeate MB solutions, respectively. The pure water flux and MB rejection tests were replicated for at least three membrane samples and average values were given with standard deviations.

The surface morphology of the produced membranes was observed by scanning electron microscopy (SEM – Carl Zeiss / Gemini 300). Samples were coated with 15 nm gold palladium and coated samples images were observed with 500 x and 5000 x magnifications.

3. RESULTS AND DISCUSSION

3.1. Characterization of Carbon-based Material

The elemental contents of CBM0 and CBM were listed in Table 1. As expected, CBM has a higher N content than CBM0 since it was functionalized by a nitrogen-containing acid. The higher C content of CBM could be attributed to the higher carbonization degree of CBM due to the presence of acids used in hydrothermal carbonization process.

The specific surface area, pore volume and pore size of the CBM0 and CBM obtained based on the N_2 adsorption-desorption datas were also given in Table 1. The specific surface area of CBM was expanded from 19.0 to 258.0 m^2/g (Table 1). This huge increase in the surface area of the CBM could attributed the presence of the acids in the hydrothermal carbonization of this sample. It is known from the literature the presence of such acids in the hydrothermal

Table 1 Textural properties and elemental compositions of carbon materials

	BET surface area (m^2/g)	***Pore Volume (cm^3/g)***	***Pore width (nm)***	***Total acid sites (mmol/g)***	***C***	***H***	***N***	***O ****
					(wt. %)			
CBM0	19.0	0.004	0.91	0.04	61.5	4.2	-	34.3
CBM	258.0	0.01	1.31	0.30	67.4	4.1	2.8	25.7

Calculated by difference, approximately value O% = 100 − [C% + H% + N%]

carbonization promote the dehydration reaction, decrease carbon aggregation thus resulted in a significant increase in specific surface area [28-30]. The CBM could be classified as mesoporous material with average pore size in fall in the range of 2–50 nm.

The FTIR analysis was used to reveal possible functional groups of CBM0 and CBM. The broad peaks located between 3000–3600 cm^{-1} were related to O–H stretching modes of the carboxyl and phenolic hydroxyl groups. The peaks at 2921 and 812 cm^{-1} corresponded to the stretching vibration of aliphatic and aromatic C–H bond [24, 31]. The band at 1700 cm^{-1} was related to the absorption of C=O bonds from -COOH groups. The peak located at 1600 cm^{-1} corresponded to the C=C stretching in the aromatic ring skeleton and this band strength of the CBM was higher than CBM0 which could be ascribed to an increase in aromaticity [21]. A distinct band at 1400 cm^{-1} was assigned to the O=S=O stretching vibration in $–SO_3H$ group. And, a new broad band appeared between 1060 to 1262 cm^{-1} could be attributed to $-SO_3$ symmetric vibration which could also be ascribed to the substitute of acidic $–SO_3H$ groups [32].

3.2. Characterization of CBM Added Membranes

3.2.1. Morphological Characteristics of the Produced Membranes

It is known in the literature that the acetone ratio used in the DMF/acetone solution system is effective in the formation of nanofibers while obtaining the nanofiber surface from PVDF. If the volatile organic solvent ratio in the solvent mixture is low, film formation takes place instead of the nanofiber surface [33]. Although the weight ratio of acetone to DMF ratio was kept 1:1 in this study, no fibrous surface formation occurred in the undoped sample. Carbon-based materials are known to increase conductivity [15, 34, 35]. When CBM was added to the electrospinning solution, it increased the conductivity and regulated the jet behavior, and thus fiber formation occurred in the doped structures. In Figure 1, surface images of M-1 and M-3 membranes are given with 500x and 5000x magnifications. While M-0 formed a completely flat film surface, a structure consisting of fiber and film mixture was obtained after the addition of 1% CBM as seen in Figure 1. When the additive ratio is further increased, a smooth jet formation is achieved and a nanofiber surface consisting of finer fibers is provided with diameter of 592±114 nm. These results were also confirmed by flux tests.

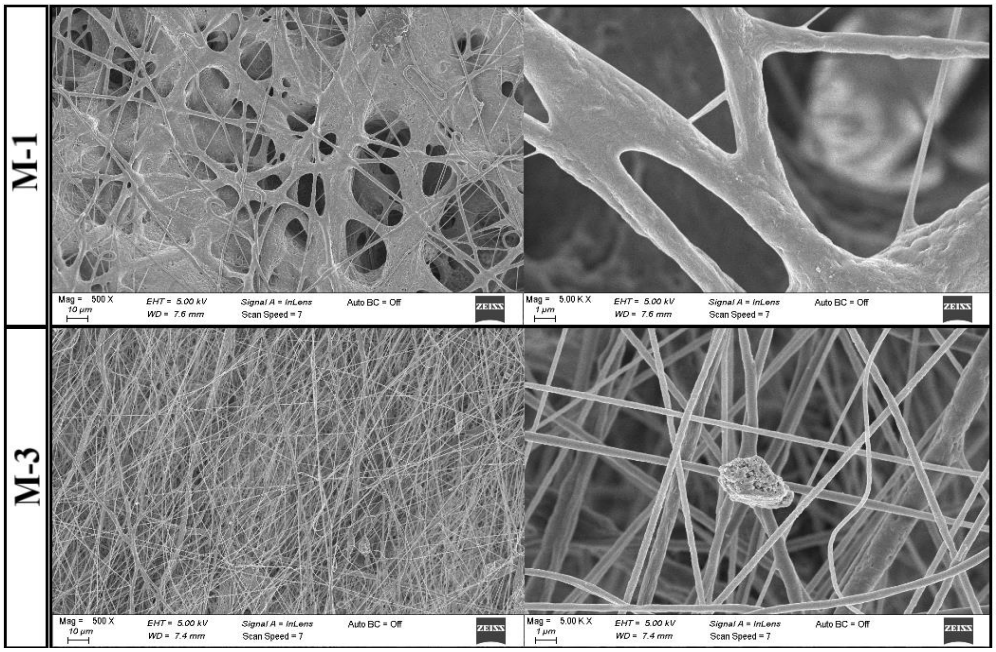

Figure 1 SEM images of the produced membranes

3.2.2. FTIR Characterization of the Produced Membranes

FTIR spectra of neat PVDF and CBM added PVDF membranes were given in Figure 2. The addition of the CBM did not cause an additional band formation, but changed the crystallization behavior of the membrane. In order to determine the variation of the specific crystalline phases of the produced membranes, the spectra were examined in the region between 400 cm^{-1} to 1000 cm^{-1}. While the bands at 840, 509, and 473 cm^{-1} were characteristic for β phase, the bands at 974, 795, 762, 613, and 531 cm^{-1} were associated with α phase crystals of the PVDF. It was observed that the M-3 demonstrated the highest band intensities for β phase bands and also it has the second highest band intensities for α phase associated bands. This showed that the most crystallization occurred in M-3, which was also confirmed by DSC analysis. The band at 473 cm^{-1} associated with the β phase was observed only in M-3 and M-2. This result showed that CBM addition to the membrane structure increases the formatiın of the β phase crystals. The relative amount of β phase was quantified using Lambert-Beer law [36] by considering the relative intensity of absorption bands at 762 cm^{-1} (α phase) and 840 cm^{-1} (β phase). The $F(\beta)/F(\alpha)$ was calculated by the following equation,

$$\frac{F(\beta)}{F(\alpha)} = \frac{A_\beta^{840}}{1.26\, A_\alpha^{762}} \quad (3)$$

where A_α and A_β are the absorbed intensity at 762 and 840 cm^{-1}, respectively. β/α phase ratio of the M-0, M-1, M-2, and M-3 were calculated as 0.845, 1.0248, 1.752, and 1.496, respectively. The addition of CBM increased the beta phase of the membrane, but the β/α phase ratio of M-3 was lower than that of M-2, as the alpha phase fraction was also increased when the addition amount was increased to 3%.

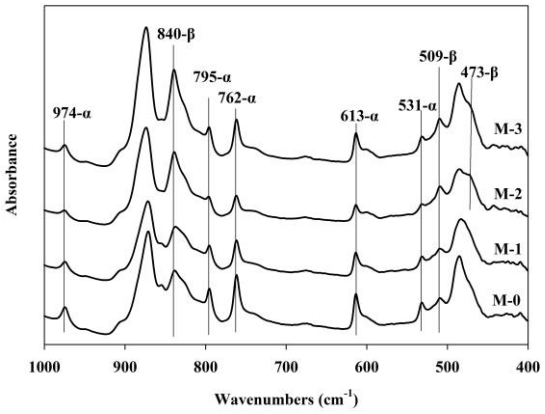

Figure 2 FTIR spectra of produced membranes

3.2.3. Thermal Properties and Crystallinity of the Produced Membranes

The DSC thermograms of the neat PVDF and CBM added PVDF membranes were given in Figure 3. All membranes demonstrated a similar melting temperature at approximately 168°C, indicating the CBM addition did not cause disruption in the thermal transition of the PVDF. Melting peaks of the α- and β-crystals appear to be superimposed at that temperature, in all membrane thermograms. However, the crystallinity of the membranes differed with the addition of the CBM. The degree of crystallinity of the produced membranes were calculated by the fusion enthalpy of the PVDF crystal (ΔH_f°=105 J/g). The melting temperature and crystallinity of the produced membranes were summarized in Table 2. It is know in literature, the structure, dimension of the nanoparticle and the addition amount of this material to the solution can cause difference of the obtain fiber crystallinity [15, 37]. As seen in the table, while 1% CBM additive did not affect the crystallization behavior of the membrane, when the additive rate was increased to 2%, the crystallization rate of the membrane decreased from 64% to 58.13%, although CBM further increased conductivity and so facilitated fiber drawing. This can be explained by the fact that the conductivity increase provided by the CBM additive did not reach the level to orient the fibers. As a result of further increase in the additive ratio, the orientation of the fibers increased with the increased conductivity and thus the highest crystallization was observed in M-3 (82.68%). Similar results are also found in the literature, Nasır et al [15] produced carbon black/PVDF copolymer nanocomposites, 5% carbon black added PVDF nanofibers showed more crystallization than 1% carbon black added fibers.

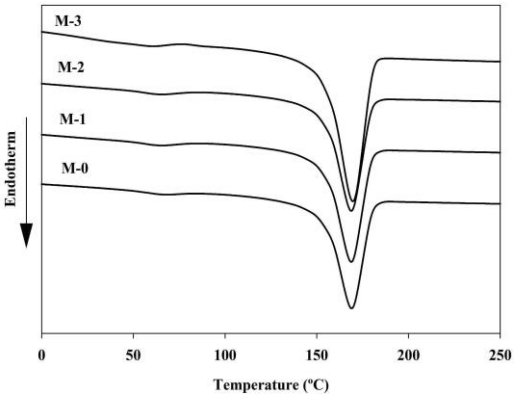

Figure 1 DSC thermogram of the produced membranes

Table 2 Thermal properties and crystallinity of the produced membranes

	Tm (°C)	*Crystallinity (%)*
M-0	168.98	64.01
M-1	168.76	64.98
M-2	168.76	58.13
M-3	169.17	82.68

3.2.4. Permeability Properties of the Produced Membranes

The pure water flux and MB dye rejection performances of the neat and CBM added membranes were given in Figure 4. As explained in the SEM results (Figure 1), M-0 formed a flat film surface. Therefore, permeation tests could not be applied to this membrane. The addition of CBM to the electrospinning solution increased the electrical conductivity, regulated the jet behavior and made it possible to obtain nanofiber surfaces as seen in the SEM images. More importantly, it thus created a porous surface structure, making the resulting structure suitable for membrane applications. As can be seen in the SEM images, a complete nanofiber structure has not yet been obtained at the 1% CBM contribution. For this reason, as seen in Figure 4, the M-1 membrane gives a very low pure water flux value of 22.1 L/m^{2}h. It is known in the literature, the addition of carbon based materials improve the water flux performance of the electrospun PVDF membranes [38, 39]. Similar to literature, when the CBM additive ratio was increased to 2%, a surface consisting entirely of

nanofibers were obtained, and thus a great increase in flux performance was obtained with the increase in porosity. However, as can be seen in Figure 4, the MB rejection performance of the M-2 decreased from 100% to 64% compared to M-1, since the film part of the M-1 is also effective in rejection of the dye. By increasing the CBM additive ratio, the pure water flux performance of the membrane increased further, as a surface consisting of more nano fibers was achieved. At the same time, a significant increase was achieved in the dye rejection performance as the dye adsorber additive ratio was increased.

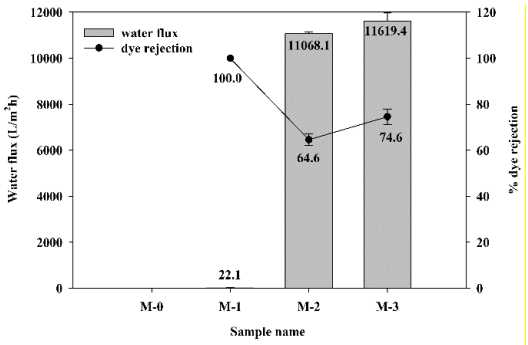

Figure 2 Water flux and dye rejection performances of the produced membranes

4. CONCLUSION

Acid functionalized CBM with high adsorption capacity were produced from cellulosic biowaste by a two-step carbonization process. Electrospun PVDF membranes, in which the produced CBM is doped in various ratios, were produced successfully. It was observed that the CBM additive increasing the conductivity during electrospinning supports nanofiber drawing. While flat film structures were formed in M-0 and M-1 membranes, nanofibrous membrane structures were obtained in M-2 and M-3 with the increase in the additive ratio. This was confirmed by SEM images, water flux and dye rejection results. M-0 and M-1, which form a flat film surface, showed very low water flux values. The M-3 showed the highest water flux performance, while the MB rejection rate also increased by 10% compared to the M-2. This result showed that the CBM addition promotes finer fiber spinning and the additive works actively in the adsorption of cationic dyestuffs. In addition, FTIR and DSC results showed that the CBM addition supports the formation of regular crystals in the membrane structure, thus enabling the production of more durable membranes.

Funding
The author (s) has no received any financial support for the research, authorship or publication of this study.

Authors' Contribution
The authors contributed equally to the study.

The Declaration of Conflict of Interest/ Common Interest
No conflict of interest or common interest has been declared by the authors.

The Declaration of Ethics Committee Approval
This study does not require ethics committee permission or any special permission.

The Declaration of Research and Publication Ethics
The authors of the paper declare that they comply with the scientific, ethical and quotation rules of SAUJS in all processes of the paper and that they do not make any falsification on the data collected. In addition, they declare that Sakarya University Journal of Science and its editorial board have no responsibility for any ethical violations that may be encountered, and that this study has not been evaluated in any academic publication environment other than Sakarya University Journal of Science.

REFERENCES

[1] E. Santoso, R. Ediati, Y. Kusumawati, H. Bahruji, D. O. Sulistiono, D. Prasetyoko, "Review on recent advances of carbon based adsorbent for methylene blue removal from

wastewater," Materials Today Chemistry, vol. 16, no. 100233, 2020.

[2] J. Li, L. Huang, X. Jiang, L. Zhang, X. Sun, "Preparation and characterization of ternary Cu/Cu_2O/C composite: An extraordinary adsorbent for removing anionic organic dyes from water," Chemical Engineering Journal, vol. 404, no. 127091, 2021.

[3] K. B Tan, M. Vakili, B. A. Horri, P. E. Poh, A. Z. Abdullah, B. Salamatinia, "Adsorption of dyes by nanomaterials: recent developments and adsorption mechanisms," Separation and Purification Technology, vol. 150, pp. 229-242, 2015.

[4] P. Verma, S. K. Samanta, "Microwave-enhanced advanced oxidation processes for the degradation of dyes in water," Environmental chemistry letters, vol. 16, no. 3, pp. 969-1007, 2018.

[5] J. Zhao, H. Liu, P. Xue, S. Tian, S. Sun, X. Lv, "Highly-efficient PVDF adsorptive membrane filtration based on chitosan@ CNTs-COOH simultaneous removal of anionic and cationic dyes," Carbohydrate Polymers, vol. 274, no. 118664, 2021.

[6] H. D. Bouras, Z. Isik, E. B. Arikan, N. Bouras, A. Chergui, H. C. Yatmaz, N. Dizge, "Photocatalytic oxidation of azo dye solutions by impregnation of ZnO on fungi," Biochemical Engineering Journal, vol. 146, pp. 150-159, 2019.

[7] A. Nasar, F. Mashkoor, "Application of polyaniline-based adsorbents for dye removal from water and wastewater—a review," Environmental Science and Pollution Research, vol. 26, no. 6, pp. 5333-5356, 2019.

[8] F. Demirci, A. Aydın, M. Orhan, H. B. Koçer, "Production of ultrafiltration membranes exhibiting antibacterial properties by the incorporation of novel N-halamine copolymers," Journal of Applied Polymer Science, vol. 139, no. 31, no. e52727, 2022.

[9] J. Wang, Q. Zhang, X. Shao, J. Ma, G. Tian, "Properties of magnetic carbon nanomaterials and application in removal organic dyes," Chemosphere, vol. 207, pp. 377-384, 2018.

[10] F. Baskoro, S. R. Kumar, S. J. Lue, "Grafting thin layered graphene oxide onto the surface of nonwoven/PVDF-PAA composite membrane for efficient dye and macromolecule separations," Nanomaterials, vol. 10, no. 4, pp. 792, 2020.

[11] L. Zhou, Y. He, H. Shi, G. Xiao, S. Wang, Z. Li, J. Chen, "One-pot route to synthesize HNTs@ PVDF membrane for rapid and effective separation of emulsion-oil and dyes from waste water," Journal of hazardous materials, vol. 380, no. 120865, 2019.

[12] Y. Song, Y. Wang, N. Zhang, X. Li, X. Bai, T. Li, "Quaternized carbon-based nanoparticles embedded positively charged composite membranes towards efficient removal of cationic small-sized contaminants," Journal of Membrane Science, vol. 630, no. 119332, 2021.

[13] F. Liu, N. A. Hashim, Y. Liu, M. M. Abed, K. Li, "Progress in the production and modification of PVDF membranes," Journal of Membrane Science, vol. 375, no. 1-2, pp. 1-27, 2011.

[14] S. Mohamadi, N. Sharifi-Sanjani, "Crystallization of PVDF in graphene-filled electrospun PVDF/PMMA

nanofibers processed at three different conditions," Fibers and Polymers, vol. 17, no. 4, pp. 582-592, 2016.

[15] M. Nasir, R. I. Sugatri, P. P. P. Asri, F. Dara, "Nanostructure and surface characteristic of electrospun carbon black/PVDF copolymer nanocomposite," Journal of Silicate Based and Composite Materials, vol. 70, no. 209-213, 2018.

[16] G. Yang, D. Zhang, G. Zhu, T. Zhou, M. Song, L. Qu, K. Xiong, H. Li, "A Sm-MOF/GO nanocomposite membrane for efficient organic dye removal from wastewater," RSC Advances, vol. 10, no. 14, pp. 8540-8547, 2020.

[17] S. Tahazadeh, T. Mohammadi, M. A. Tofighy, S. Khanlari, H. Karimi, H. B. M. Emrooz, "Development of cellulose acetate/metal-organic framework derived porous carbon adsorptive membrane for dye removal applications," Journal of Membrane Science, vol. 638, no. 119692, 2021.

[18] M. A. Lalabadi, H. Peyman, H. Roshanfekr, S. Azizi, M. Maaza, "Polyethersulfone nanofiltration membrane embedded by magnetically modified MOF (MOF@ Fe3O4): fabrication, characterization and performance in dye removal from water using factorial design experiments," Polymer Bulletin, pp. 1-21, 2022.

[19] A. K. Shukla, J. Alam, F. A. A. Ali, M. Alhoshan, "Efficient soluble anionic dye removal and antimicrobial properties of ZnO embedded-Polyphenylsulfone membrane," Water and Environment Journal, vol. 35, no. 2, pp. 670-684, 2021.

[20] S. Gholami, J. L. Llacuna, V. Vatanpour, A. Dehqan, S. Paziresh, J. L. Cortina, "Impact of a new functionalization of multiwalled carbon nanotubes on antifouling and permeability of PVDF nanocomposite membranes for dye wastewater treatment," Chemosphere, vol. 294, pp. 133699, 2022.

[21] M. M. Fu, C. H. Mo, H. Li, Y. N. Zhang, W. X. Huang, M. H. Wong, "Comparison of physicochemical properties of biochars and hydrochars produced from food wastes," Journal of Cleaner Production, vol. 236, no. 117637, 2019.

[22] X. Zhang, Y. Zhang, H. H. Ngo, W. Guo, H. Wen, D. Zhang, C. Li, L. Qi, "Characterization and sulfonamide antibiotics adsorption capacity of spent coffee grounds based biochar and hydrochar," Science of the Total Environment, vol. 716, no. 137015, 2020.

[23] A. Jain, R. Balasubramanian, M. P. Srinivasan, "Hydrothermal conversion of biomass waste to activated carbon with high porosity: A review," Chemical Engineering Journal, vol. 283, pp. 789-805, 2016.

[24] R. O. Araujo, J. da Silva Chaar, L. S. Queiroz, G. N. da Rocha Filho, C. E. F. da Costa, G. C da Silva, R. Landers, M. J. Costa, A. A. Gonçalves, L. K. de Souza, "Low temperature sulfonation of acai stone biomass derived carbons as acid catalysts for esterification reactions," Energy Conversion and Management, vol 196, pp. 821-830, 2019.

[25] T. Foyle, L. Jennings, P. Mulcahy, "Compositional analysis of lignocellulosic materials: Evaluation of methods used for sugar analysis of waste paper and straw," Bioresource Technology, vol. 98, no. 16, pp. 3026-3036, 2007.

[26] M. M. A. D. Maciel, K. C. C Benini, H. J. C. Voorwald, M. O. H. Cioffi, "Obtainment and characterization of nanocellulose from an unwoven industrial textile cotton waste: Effect of acid hydrolysis conditions," International Journal of Biological Macromolecules, vol. 126, pp. 496-506, 2019.

[27] C. Samori, A. Parodi, E. Tagliavini, P. Galletti, "Recycling of post-use starch-based plastic bags through pyrolysis to produce sulfonated catalysts and chemicals," Journal of Analytical and Applied Pyrolysis, vol. 155, no. 105030, 2021.

[28] R. F. Susanti, A. A. Arie, H. Kristianto, M. Erico, G. Kevin, H. Devianto, "Activated carbon from citric acid catalyzed hydrothermal carbonization and chemical activation of salacca peel as potential electrode for lithium ion capacitor's cathode", Ionics, vol. 25, pp. 3915-3925, 2019.

[29] H. Simsir, N. Eltugral, S. Karagoz, "Effects of acidic and alkaline metal triflates on the hydrothermal carbonization of glucose and cellulose," Energy & Fuels, vol. 33, no. 8, pp. 7473-7479, 2019.

[30] Z. Hoseinabadi, S. A. Pourmousavi, "Synthesis of Starch Derived Sulfonated Carbon-based Solid Acid as a Novel and Efficient Nanocatalyst for the Synthesis of Dihydropyrimidinones," Warasan Khana Witthayasat Maha Witthayalai Chiang Mai, vol. 46, no. 1, pp. 132-143, 2019.

[31] Z. Liu, Z. Liu, "Comparison of hydrochar-and pyrochar-based solid acid catalysts from cornstalk: Physiochemical properties, catalytic activity and deactivation behavior," Bioresource Technology, vol. 297, no. 122477, 2020.

[32] R. S. Salama, S. M. El-Bahy, M. A. Mannaa, "Sulfamic acid supported on mesoporous MCM-41 as a novel, efficient and reusable heterogenous solid acid catalyst for synthesis of xanthene, dihydropyrimidinone and coumarin derivatives," Colloids and Surfaces A: Physicochemical and Engineering Aspects, vol. 628, no. 127261, 2021.

[33] Y. J. Hwang, S. Choi, H. S. Kim, "Structural deformation of PVDF nanoweb due to electrospinning behavior affected by solvent ratio," e-Polymers, vol. 18, no. 4, pp. 339-345, 2018.

[34] J. Hwang, J. Muth, T. Ghosh, "Electrical and mechanical properties of carbon-black-filled, electrospun nanocomposite fiber webs," Journal of Applied Polymer Science, vol. 104 no. 4, pp. 2410-2417, 2007.

[35] E. Tarasova, A. Byzova, N. Savest, M. Viirsalu, V. Gudkova, T. Maertson, A. Krumme, "Influence of preparation process on morphology and conductivity of carbon black-based electrospun nanofibers," Fullerenes, Nanotubes and Carbon Nanostructures, vol. 23, no. 8, pp. 695-700, 2014.

[36] M. M. Tao, F. Liu, B. R. Ma, L. X. Xue, "Effect of solvent power on PVDF membrane polymorphism during phase inversion," Desalination, vol. 316, pp. 137-145, 2013.

[37] R. Moradi, J. Karimi-Sabet, M. Shariaty-Niassar, M. A. Koochaki, "Preparation and characterization of polyvinylidene fluoride/graphene superhydrophobic fibrous films",

Polymers, vol. 7, no. 8, pp. 1444-1463, 2015.

[38] N. Mehranbod, M. Khorram, S. Azizi, N. Khakinezhad, "Modification and superhydrophilization of electrospun polyvinylidene fluoride membrane using graphene oxide-chitosan nanostructure and performance evaluation in oil/water separation", Journal of Environmental Chemical Engineering, vol. 9, no. 5, pp. 106245, 2021.

[39] J. A. Park, A. Nam, J. H. Kim, S. T. Yun, J. W. Choi, S. H. Lee, "Blend-electrospun graphene oxide/Poly (vinylidene fluoride) nanofibrous membranes with high flux, tetracycline removal and anti-fouling properties", Chemosphere, vol. 207, pp. 347-356, 2018.